Brain Temporal-Spectral Functional Variability Reveals Neural Improvements of DBS Treatment for Disorders of Consciousness

Jiewei Lu, Jingchao Wu, Zhilin Shu, Xinyuan Zhang, Haitao Li, Siquan Liang, Jianda Han, *Member, IEEE*, and Ningbo Yu, *Member, IEEE*

***Abstract*— Deep brain stimulation (DBS) is establishing itself as a promising treatment for disorders of consciousness (DOC). Measuring consciousness changes is crucial in the optimization of DBS therapy for DOC patients. However, conventional measures use subjective metrics that limit the investigations of treatment-induced neural improvements. The focus of this study is to analyze the regulatory effects of DBS and explain the regulatory mechanism at the brain functional level for DOC patients. Specifically, this paper proposed a dynamic brain temporal-spectral analysis method to quantify DBS-induced brain functional variations in DOC patients. Functional near-infrared spectroscopy (fNIRS) that promised to evaluate consciousness levels was used to monitor brain variations of DOC patients. Specifically, a fNIRS-based experimental procedure with auditory stimuli was developed, and the brain activities during the procedure from thirteen DOC patients before and after the DBS treatment were recorded. Then, dynamic brain functional networks were formulated with a sliding-window correlation analysis of phase lag index. Afterwards, with respect to the temporal variations of global and regional networks, the variability of global efficiency, local efficiency, and clustering coefficient were extracted. Further, dynamic networks were converted into spectral representations by graph Fourier transform, and graph energy and diversity were formulated to assess the spectral global and regional variability. The results showed that DOC patients under DBS treatment exhibited increased global and regional functional variability that was significantly associated with consciousness improvements. Moreover, the functional variability in the right brain regions had a stronger correlation with consciousness enhancements than that in the left brain regions. Therefore, the proposed method well signifies DBS-induced brain functional variations in DOC patients, and the functional variability may serve as promising biomarkers for consciousness evaluations in DOC patients.**

***Index Terms*— Deep brain stimulation, disorders of consciousness, fNIRS, dynamic brain functional networks, dynamic brain temporal-spectral features, global and regional variability.**

Manuscript received 31 October 2023; revised 8 January 2024 and 10 February 2024; accepted 18 February 2024. Date of publication 22 February 2024; date of current version 27 February 2024. This work was supported in part by the National Natural Science Foundation of China under Grant U1913208, in part by Shenzhen Science and Technology Program under Grant KQTD20210811090143060, in part by the Science and Technology Program of Tianjin under Grant 21JCZDJC00170 and Grant 21JCYBJC01440, in part by the Key Scientific Research Project of Tianjin Health Commission under Grant ZD20017, in part by Tianjin Key Medical Discipline (Specialty) Construction Project, and in part by the Excellent Youth Team of Central Universities under Grant NKU-63231196. *(Jiewei Lu and Jingchao Wu are co-first authors.) (Corresponding authors: Siquan Liang; Jianda Han; Ningbo Yu.)*

This work involved human subjects or animals in its research. Approval of all ethical and experimental procedures and protocols was granted by the Ethics Committee of Tianjin Huanhu Hospital, Tianjin, China, under Application No. 2020-105, and performed in line with the Declaration of Helsinki.

Jiewei Lu, Zhilin Shu, and Xinyuan Zhang are with the College of Artificial Intelligence, Nankai University, Tianjin 300350, China.

Jingchao Wu, Haitao Li, and Siquan Liang are with the Department of Neurosurgery, Tianjin Huanhu Hospital, Tianjin 300350, China (e-mail: liangsiquan@163.com).

Jianda Han and Ningbo Yu are with the College of Artificial Intelligence, Tianjin Key Laboratory of Intelligent Robotics, and the Engineering Research Center of Trusted Behavior Intelligence, Ministry of Education, Nankai University, Tianjin 300350, China, and also with the Institute of Intelligence Technology and Robotic Systems, Shenzhen Research Institute of Nankai University, Shenzhen 518083, China (e-mail: hanjianda@nankai.edu.cn; nyu@nankai.edu.cn).

Digital Object Identifier 10.1109/TNSRE.2024.3368434

I. Introduction

DISORDERS of consciousness (DOC) refer to a broad spectrum of neurologic conditions mainly characterized by impaired awareness and arousal [1]. These disorders encompass various clinical entities, including vegetative state and minimally conscious state [2], [3]. A comprehensive understanding of these conditions is essential for accurate clinical diagnosis, prognosis assessment, and treatment planning [4], [5].

Deep brain stimulation (DBS) is a promising therapeutic approach for DOC [6], involving the implantation of stimulating electrodes in the brain to modulate neural activity [7]. In [8], Schiff showed that DBS modulates behavioral responsiveness in a patient with minimally conscious state. In [9], Magrassi et al. found that DBS could improve the clinical status of patients in the vegetative state and minimally

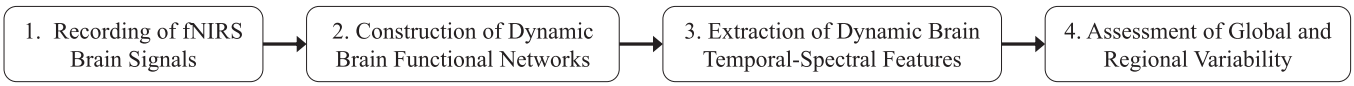

Fig. 1. The framework of the proposed method, including (1) fNIRS recording of DOC patients, (2) dynamic brain functional network construction with a sliding-window correlation analysis of phase lag index, (3) extraction of dynamic brain temporal-spectral features, and (4) global and regional variability assessment.

conscious state. In [10], Yang et al. demonstrated that DBS led to significant functional improvements of DOC patients and had better effects in patients with minimally conscious state than patients with vegetative state. Besides DBS, other treatment methods for DOC include rehabilitative therapies, sensory stimulation, pharmacological interventions, etc [11], [12], [13]. Compared with these treatments, DBS allows for precise and localized stimulation of specific brain regions implicated in consciousness and has the potential to induce long-term changes in neural circuitry involved in DOC [14].

DBS has been used for the treatment of DOC. However, the specific effects of DBS for DOC patients and the underlying neural mechanism have not been well explored. Assessing DBS effects in DOC is essential in the optimization of DBS therapy for DOC patients. A number of studies tried to evaluate the performance of DBS in DOC patients with Coma Recovery Scale-Revised (CRS-R), which was powerful in the assessment and monitoring of patients with DOC [15], [16]. In addition, an effective modified CRS-R (named CRS-R index) was proposed for the diagnosis of DOC patients [17]. Compared with conventional CRS-R, CRS-R index accounted for the hierarchical structure of the individual items (auditory, visual, motor, oromotor, communication, and arousal) in the CRS-R assessment and had better diagnostic precision to distinguish between patients with vegetative state and minimally conscious state. However, CRS-R relies on the expertise and judgment of doctors and is prone to intra-rater and inter-rater variability. Moreover, CRS-R is incapable of detecting brain variations and thus has inherent limitations in assessing the state of consciousness.

A growing number of studies approached the evaluation of DBS effects for DOC patients at the brain functional level with functional magnetic resonance imaging (fMRI), electroencephalography (EEG), positron emission tomography (PET), etc [18], [19], [20], [21]. In addition, functional near-infrared spectroscopy (fNIRS), an emerging neuroimaging technique, is increasingly utilized to analyze brain functional variations of neurological disorders for its adaptability for diverse experimental setups, portability for task-related measurement, robustness to motion-related interference, etc [22], [23]. fNIRS monitored the cortical hemodynamic changes which occur in response to neural activity. With fNIRS, it can be observed how DBS affects the neural activity in specific brain regions implicated in regulatory mechanisms. Previous studies found that fNIRS could effectively detect DBS-induced brain functional variations in patients with Parkinson's disease [24], [25]. Moreover, fNIRS showed promise in evaluating the levels of consciousness in DOC patients [26], [27], [28]. Thus, fNIRS could be applied to analyze the regulatory mechanisms of DBS in DOC patients.

In our previous work, we assessed the DBS-induced brain functional variations in DOC patients with fNIRS-based functional connectivity analysis [29]. However, the investigations of network dynamics remained limited. Networks dynamics characterized the temporal expression of brain functional networks and was associated with a variety of neurological disorders [30], [31]. Specifically, network dynamics was related to the levels of consciousness and contributed to investigating the underlying neural mechanism of DOC [32], [33]. In [34], Cai et al. found that the loss of consciousness was associated with the declined spatial and temporal variability of dynamic functional networks. In [35], López-González showed that the loss of consciousness reduced network interactions and heterogeneity of brain dynamics. Thus, the enhanced network dynamics was related to the improvements of consciousness levels and promising in characterizing DBS-induced improvements at the brain functional level among DOC patients.

This paper proposed an analysis method to clarify the DBS-induced improvements at the brain functional level for DOC patients with respect to brain network dynamics. Specifically, dynamic brain features were extracted to quantify the functional variability in the temporal and spectral representations of brain functional networks. The results showed that brain temporal-spectral functional variability well signified brain functional variations of DBS treatment for DOC patients and could be applied to evaluate consciousness in DOC patients.

II. Methods

The proposed dynamic brain temporal-spectral analysis method was presented in Figure 1. fNIRS recording of DOC patients during auditory stimuli was introduced first. Then, the construction of dynamic brain functional networks was detailed. Afterwards, the extraction of dynamic brain temporal-spectral features for the assessment of global and regional functional variability was presented.

A. Participants

This study obtained ethical approval from the Ethics Committee of Tianjin Huanhu Hospital, Tianjin, China (No. 2020-105). Before the experiment, written informed consents were provided by caregivers of the patients. Thirteen DOC patients with DBS surgery were included in the experiment, as depicted in Table I. The inclusion criteria of DOC patients were: (1) age between 18 and 75 years; (2) a minimum duration of 6 months of stable DOC for patients with traumatic injuries and 3 months for those with non-traumatic injuries; (3) intact thalamus in the surgical side. The exclusion criteria were: (1) deafness; (2) psychiatric or neurological

TABLE I
CLINICAL CHARACTERISTICS OF DOC PATIENTS WITH DBS TREATMENT

Patient	Age	Sex	Pathogeny	Duration of Stable DOC (months)	CRS-R Score	Clincial Diagnosis	DBS Target
P1	48	Male	Trauma	18	5	VS[a]	Right CM-PF[c]
P2	37	Male	Trauma	12	5	MCS-[c]	Right CM-PF
P3	60	Male	Trauma	7	3	VS	Right CM-PF
P4	46	Male	Trauma	6	4	VS	Bilateral CM-PF
P5	72	Female	Hypothalamus Hemorrhage	3	2	VS	Right CM-PF
P6	75	Female	Basal Ganglia Hemorrhage	7	4	VS	Bilateral CM-PF
P7	61	Male	Cerebellar Hemorrhage	3	4	VS	Bilateral CM-PF
P8	53	Male	Brainstem Hemorrhage	6	5	MCS-	Bilateral CM-PF
P9	59	Male	Brainstem Hemorrhage	3	2	VS	Bilateral CM-PF
P10	55	Male	Brainstem Infarction	3	3	VS	Bilateral CM-PF
P11	69	Female	Brainstem Infarction	6	4	VS	Bilateral CM-PF
P12	58	Male	Trauma	6	4	VS	Bilateral CM-PF
P13	69	Female	Trauma	6	2	VS	Bilateral CM-PF

a: Vegetative state.
b: Minimally conscious state minus.
c: Centromedian-parafascicular.

disorders; (3) infectious or metabolic brain injury; (4) locked-in syndrome; (5) use of sedatives; (6) needing assistance with breathing or circulation; (7) impairments of hearing and eye movements. Stable DOC states of patients were determined through multiple CRS-R evaluations conducted by two experienced specialists.

Patients with cranial defects on the left side of the nucleus were subjected to treatment targeting the right centromedian-parafascicular (CM-PF) nuclei while patients without cranial defects underwent treatment targeting the bilateral CM-PF nuclei. The implantation procedure of the Permanent Electrode leads (PINS L301 model, PINS Inc., Beijing, China) was carried out under the guidance of the Leksell frame. With the utilization of targeting software (Framelink 5.1, Medtronic, Minneapolis, MN, USA), the surgical team planned the anatomical target and identified the optimal trajectory by magnetic resonance imaging (MRI) and computed tomography (CT) scans. Lead DBS software was applied to reconstruct the relationship between the electrode and the nucleus, ensuring that the electrode contacts were within the nucleus of CM-PF [36]. From the third day after the DBS surgery, monopolar stimulation was administered continuously with a frequency of 100 Hz and a pulse width of 210 ms. Doctors gradually increased the voltage without producing any side effects, such as facial tension, limb hypertonia, and spasms [9]. The voltage ranged from 2.5 V to 3.5 V, depending on the patient's condition. Stimulation was applied for 15 minutes every 30 minutes throughout the daytime.

B. Recording of fNIRS Brain Signals During the Experimental Procedures

fNIRS brain signals were captured by a portable Nirsmart system (Danyang Huichuang Medical Equipment Co., Ltd China) at a sampling rate of 11 Hz. The wavelengths of the Nirsmart system were 730 nm and 850 nm. Eighteen sources and fourteen detectors were symmetrically placed at bilateral hemispheres, covering frontal lobe, parietal lobe, and occipital lobe. Each pair of source and detector produced an fNIRS channel, and a total of 34 channels were generated in this study, as illustrated in Figure 2.

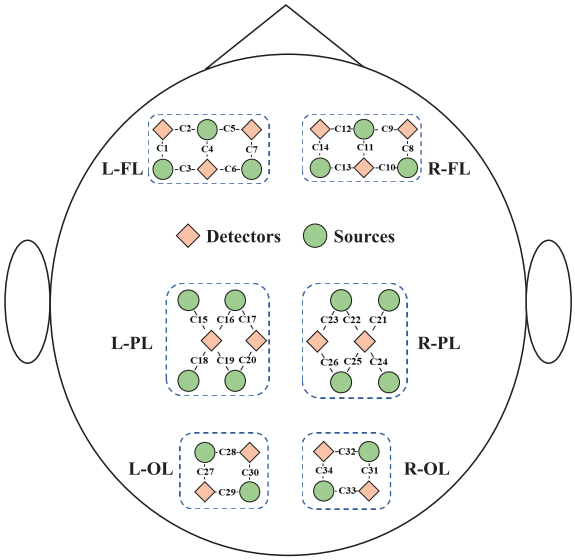

Fig. 2. Optode distribution. Thirty-two optodes including eighteen sources and fourteen detectors were symmetrically distributed in frontal cortex (FL), parietal lobe (PL), and occipital lobe (OL). Each pair of source and detector produces an fNIRS channel, and a total of 34 channels are generated in this study. C*i* indicates the *i*-th fNIRS channel.

With the portable fNIRS system, an experimental procedure was developed according to the CRS-R auditory subscore, involving the utilization of auditory stimuli. Previous studies found that auditory stimuli could effectively stimulate the brain of DOC patients [37], [38], [39]. The experimental procedure consisted of: (1) an auditory stimuli trial under the Pre stage (two days before the DBS surgery), and (2) an auditory stimuli trial under the Post stage (one month after the surgery).

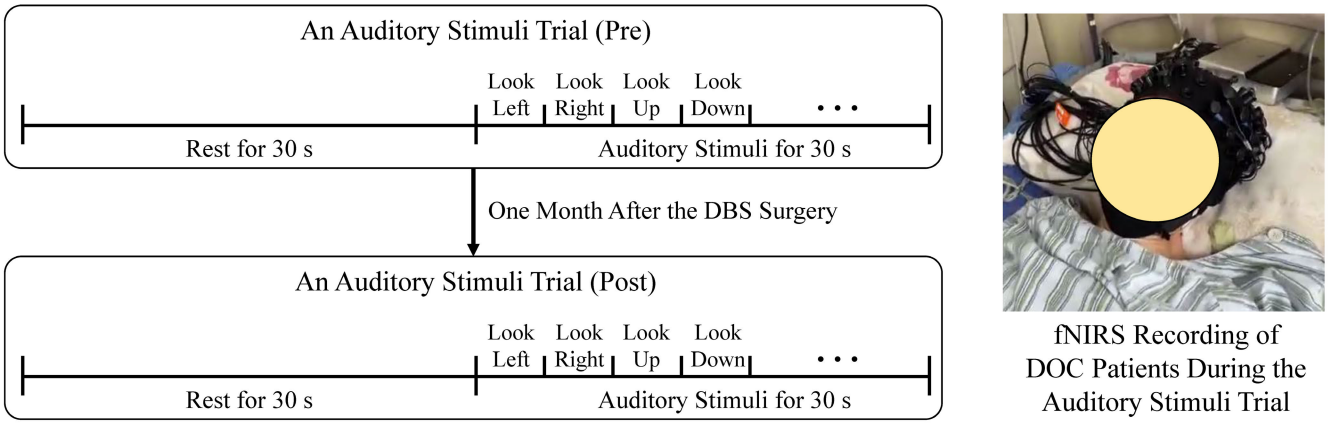

Fig. 3. The experimental procedures. fNIRS brain signals were recorded under the Pre (two days before the DBS surgery) and Post (one month after the DBS surgery) stages. The auditory stimuli trial included a rest of 30 s and an auditory stimuli of 30 s that consisted of recursive sequential instructions from one specialist to look left, right, up, and down. The instructions were delivered at a standard speaking rate, without any intervening pauses.

The auditory stimuli trial included a rest of 30 s and an auditory stimuli of 30 s and was performed in a quiet ward. The auditory stimuli consisted of recursive sequential instructions from one specialist to look left, right, up, and down. The instructions were administered at a standard speaking rate, devoid of any interposed pauses. Another specialist evaluated the response of patients to the auditory stimuli to examine whether the instructions elicited corresponding ocular movements. The experimental procedure was illustrated in Figure 3.

The recorded fNIRS signals during the experimental procedure were preprocessed with the following steps: (1) Motion artifacts were detected by combining a time window of 0.5 s and two thresholds. The first threshold was the standard deviation and set as 6. The second threshold was amplitude and set as 0.5. Motion artifacts were defined as the data within specific time windows, of which the standard deviation exceeds the first threshold or the peak amplitude exceeds the second threshold. The detected artifacts were corrected by cubic spline interpolation [40], [41]. (2) Physiological noises (such as cardiac and respiration) were filtered by a 0.01-0.2 Hz bandpass filter [30], [42], [43]. (3) The modified Beer-Lambert law was applied to transform the filtered signals into the concentration changes of oxyhemoglobin [44]. (4) Visual inspection was performed for the examination of signal quality. The channels located in the occipital lobe for P4 and P10, as well as channel 14 for P10 in the Pre stage, were excluded due to their poor signal quality.

C. Dynamic Brain Functional Networks

Dynamic brain functional networks were constructed for the analysis of time-varying coupling between different brain regions. Specially, the preprocessed signals were separated into multiple pieces using a sliding window with a size of 20 s and a step of 1 s. For each piece, the Hilbert transformation c_{hi} of each separated channel signal c_i at time t was computed as:

$$c_{hi}(t) = \frac{1}{\pi} C_{pr} \int_{-\infty}^{+\infty} \frac{c_i(\tau)}{t-\tau} d\tau \tag{1}$$

where C_{pr} was the Cauchy principle value. The phase difference $\triangle\phi$ at time t between c_i and c_j was calculated as:

$$\triangle\phi_{c_i,c_j}(t) = |\arctanh\frac{c_{hi}(t)}{c_i(t)} - \arctanh\frac{c_{hj}(t)}{c_j(t)}| \tag{2}$$

Then the phase lag index P_{c_i,c_j} was calculated as:

$$P_{c_i,c_j} = |\frac{1}{T}\sum_{t=1}^{T} sign(\triangle\phi_{c_{hi},c_{hj}}(t))| \tag{3}$$

where T denoted the length of separated channel signals. $sign(\cdot)$ indicated the signum function. P_{c_i,c_j} ranged from 0 (the weakest correlation) to 1 (the strongest correlation). The brain functional network B_{fn} of each piece was construct with P_{c_i,c_j} from all pairs of separated channel signals:

$$B_{fn} = \begin{bmatrix} P_{c_1,c_1} & P_{c_1,c_2} & \cdots & P_{c_i,c_{N_c}} \\ P_{c_2,c_1} & P_{c_2,c_2} & \cdots & P_{c_2,c_{N_c}} \\ \vdots & \vdots & \ddots & \vdots \\ P_{c_{N_c},c_1} & P_{c_{N_c},c_2} & \cdots & P_{c_{N_c},c_{N_c}} \end{bmatrix} \tag{4}$$

where N_c indicated the channel number. B_{fn} was undirected, i.e. $\forall i, j, P_{c_i,c_j} = P_{c_j,c_i}$.

D. Dynamic Brain Temporal-Spectral Features

Dynamic brain temporal-spectral features were extracted to quantify the global and local functional variability and utilized to analyze DBS-induced brain functional variations in DOC patients.

1) Brain Temporal Features: Three brain graph features including global efficiency, local efficiency, and clustering coefficient were applied for the characterization of brain functional networks. Specifically, global efficiency measured the integration of brain networks and was calculated as:

$$GE = \frac{1}{N_c}\sum_{i\in C}\frac{\sum_{j\in C, j\neq i} d_{ij}^{-1}}{N_c - 1} \tag{5}$$

where N_c denoted the channel number, C was the channel set. d_{ij} was the shortest path length between the i-th and

j-th channels. Local efficiency and clustering coefficient assessed the segregation of the networks and were computed as:

$$LE_{Re} = \frac{1}{N_{Re}} \sum_{i \in C_{Re}} \frac{\sum_{j,h \in C_{Re}, j \neq h} a_{ij} a_{ih} d_{jh} (C_{Re}(i))^{-1}}{k_i (k_i - 1)} \quad (6)$$

$$CC_{Re} = \frac{1}{N_{Re}} \sum_{i \in C_{Re}} \frac{2t_i}{k_i (k_i - 1)} \quad (7)$$

where Re denoted the brain region and set as whole (all brain regions), L-FL (the left frontal cortex), R-FL (the right frontal cortex), L-PL (the left parietal lobe), R-PL (the right parietal lobe), L-OL (the left occipital lobe), or R-OL (the right occipital lobe). N_{Re} was the channel number in Re. C_{Re} indicated the channel set of Re. $d_{ih}(C_{Re}(i))$ represented the shortest path length between channels j and h, that contains only neighbors of channel i in C_{Re}. a_{ij} was the connection status between channels i and j in C_{Re}. k_i was the degree of channel i. t_i denoted the triangle number around channel i.

The variability of global efficiency, local efficiency, and clustering coefficient were defined as:

$$V_{GE} = \frac{1}{N_{pi} - 1} \sum_{i=1}^{N_{pi}} |GE(B^i_{fn}) - \overline{GE(B_{fn})}|^2 \quad (8)$$

$$V_{LE_{Re}} = \frac{1}{N_{pi} - 1} \sum_{i=1}^{N_{pi}} |LE_{Re}(B^i_{fn}) - \overline{LE_{Re}(B_{fn})}|^2 \quad (9)$$

$$V_{CC_{Re}} = \frac{1}{N_{pi} - 1} \sum_{i=1}^{N_{pi}} |CC_{Re}(B^i_{fn}) - \overline{CC_{Re}(B_{fn})}|^2 \quad (10)$$

where N_{pi} the number of separated pieces. $\overline{GE(B_{fn})}$, $\overline{LE_{Re}(B_{fn})}$, and $\overline{CC_{Re}(B_{fn})}$ were the mean of $GE(B_{fn})$, $LE_{Re}(B_{fn})$, and $CC_{Re}(B_{fn})$ in all pieces, respectively.

2) Brain Spectral Features: Graph spectral analysis permits the transformation of graph signals into a spectral representation (graph Fourier transform) and extraction of graph pieces associated with different modes of variations, which were of great significance in the analysis of neurological diseases [45], [46]. Moreover, it facilitates a spatial variability analysis with respect to brain connectivity patterns [47]. In this study, a brain graph was defined as $\mathcal{G} = (\mathcal{V}, B_{fn})$, where $\mathcal{V} = \{v_1, v_2, \ldots, v_{n_c}\}$ was the vertice set. The degree matrix $M_D \in \mathbb{R}^{N_c \times N_c}$ of $\mathcal{G}$ was constructed as a diagonal matrix with the i-th diagonal element $M_D^{ii} = \sum_{j=1}^{N_c} P_{ci,cj}$. The Laplacian matrix M_L was defined as $M_D - B_{fn}$ and decomposed as:

$$M_L = E \Lambda E^H \quad (11)$$

where $E = [\boldsymbol{e}_1, \boldsymbol{e}_2, \ldots, \boldsymbol{e}_{n_c}]$ is the eigenvector matrix, $\boldsymbol{e}_i$ denoted the i-th eigenvector. E^H was the Hermitian of E. Λ was the diagonal eigenvalue matrix $\Lambda = diag(\lambda_1, \lambda_2, \ldots, \lambda_{N_c}) \in \mathbb{R}^{N_c \times N_c}$, λ_i is the i-th eigenvalue for $\boldsymbol{e}_i$. The graph energy was defined as:

$$energy = \sum_{i=1}^{N_c} \lambda_i \quad (12)$$

The graph diversity (GD) was defined to quantify the changes in each brain region:

$$GD_{Re} = \sum_{k=S_{high}}^{K} \frac{\sum_{i,j \in Re, i \neq j} P_{c_i,c_j} (v^i_k - v^j_k)}{\sum_{i,j \in Re, i \neq j} P_{c_i,c_j}} \quad (13)$$

where Re indicated the brain region and set as L-FL (the left frontal cortex), R-FL (the right frontal cortex), L-PL (the left parietal lobe), R-PL (the right parietal lobe), L-OL (the left occipital lobe), or R-OL (the right occipital lobe). K was the number of eigenvectors. P_{c_i,c_j} denoted the phase lag index between the i-th and j-th channels (as defined in Equ.(3)). v^i_k represented the i-th element in the k-th eigenvector. S_{high} was set as $K - round(K/3) + 1$ and indicated the start point for the eigenvectors with high graph frequencies that were potentially associated with the high frequency DBS treatment for DOC patients in this study.

Then the graph energy variability and graph diversity variability were defined as:

$$V_{energy} = \frac{1}{N_{pi} - 1} \sum_{i=1}^{N_{pi}} |energy(B^i_{fn}) - \overline{energy(B_{fn})}|^2 \quad (14)$$

$$V_{GD_{Re}} = \frac{1}{N_{pi} - 1} \sum_{i=1}^{N_{pi}} |GD_{Re}(B^i_{fn}) - \overline{GD_{Re}(B_{fn})}|^2 \quad (15)$$

where N_{pi} the number of separated pieces. $\overline{energy(B_{fn})}$ and $\overline{GD_{Re}(B_{fn})}$ were the mean of $energy(B_{fn})$ and $GD_{Re}(B_{fn})$ in all pieces.

Distance correlation analysis was conducted to investigate the correlation between the treatment-induced changes of dynamic brain temporal-spectral features and changes of CRS-R index, an effective modified version of CRS-R scores with a linear relationship to consciousness [17]. The changes of dynamic features and CRS-R index were calculated by subtracting the values in the Post stage from the values in the Pre stage.

III. Results

A. Clinical Analysis

The CRS-R evaluations of patients were conducted three times in the Pre and Post stages. The evaluations were carried out before and after surgery by the same specialist who was blinded to the experimental results. The CRS-R scores exhibited consistency across all three assessments in all patients.

The clinical results of thirteen DOC patients were presented in Table II. After DBS treatment, four patients (P1, P2, P3, P4, P13) with trauma exhibited an increase in CRS-R scores and CRS-R index, with the increment ranging from 2 to 3 and from 2.080 to 17.720. P5 patient with hypothalamus hemorrhage had a one-point increase of CRS-R score and 1.04 increase of CRS-R index. The CRS-R score and CRS-R index of P6 patient with basal ganglia hemorrhage showed an increase of 1 and 8.340. P7 patient with cerebellar hemorrhage had a 1 and 1.04 decrease of CRS-R scores and CRS-R index. The CRS-R scores and CRS-R indexes of patients

TABLE II
CLINICAL RESULTS OF DBS TREATMENT FOR DOC PATIENTS

Patient	Pathogeny	CRS-R Score			CRS-R Index			Clincial Diagnosis	
		Pre	Post	Change	Pre	Post	Change	Pre	Post
P1	Trauma	5 (0-1-2-0-0-2)[a]	7 (0-1-2-2-0-2)	+2	3.797	5.877	+2.080	VS[b]	VS
P2	Trauma	5 (0-0-3-0-0-2)	8 (0-1-3-2-0-2)	+3	11.087	14.217	+3.130	MCS-[c]	MCS-
P3	Trauma	3 (0-0-2-0-0-1)	6 (0-1-3-0-0-2)	+3	2.413	12.127	+9.714	VS	MCS-
P4	Trauma	4 (0-0-2-0-0-2)	7 (0-3-2-0-0-2)	+3	2.747	20.467	+17.720	VS	MCS-
P5	Hypothalamus Hemorrhage	2 (0-0-0-0-0-2)	3 (0-0-1-0-0-2)	+1	0.667	1.707	+1.040	VS	VS
P6	Basal Ganglia Hemorrhage	4 (0-0-2-0-0-2)	5 (0-0-3-0-0-2)	+1	2.747	11.087	+8.340	VS	MCS-
P7	Cerebellar Hemorrhage	4 (0-0-2-0-0-2)	3 (0-0-1-0-0-2)	-1	2.747	1.707	-1.040	VS	VS
P8	Brainstem Hemorrhage	5 (0-0-3-0-0-2)	5 (0-0-3-0-0-2)	0	11.087	11.087	0.000	MCS-	MCS-
P9	Brainstem Hemorrhage	2 (0-0-0-0-0-2)	2 (0-0-0-0-0-2)	0	0.667	0.667	0.000	VS	VS
P10	Brainstem Infarction	3 (0-0-1-0-0-2)	3 (0-0-1-0-0-2)	0	1.707	1.707	0.000	VS	VS
P11	Brainstem Infarction	4 (0-1-2-0-0-1)	4 (0-1-2-0-0-1)	0	3.463	3.463	0.000	VS	VS
P12	Trauma	4 (0-1-1-0-0-2)	4 (0-1-1-0-0-2)	0	2.747	2.747	0.000	VS	VS
P13	Trauma	2 (0-0-0-0-0-2)	4 (0-0-2-0-0-2)	+2	0.667	2.747	+2.080	VS	VS

a: The sub-ratings of CRS-R score in auditory, visual, motor, oromotor, communication, and arousal.
b: Vegetative state.
c: Minimally conscious state minus.

TABLE III
THE GLOBAL EFFICIENCY VARIABILITY, LOCAL EFFICIENCY VARIABILITY, CLUSTERING COEFFICIENT VARIABILITY, AND GRAPH ENERGY VARIABILITY IN THE PRE AND POST STAGES

Patient	Global Efficiency Variability		Local Efficiency Variability[a]		Clustering Coefficient Variability[a]		Graph Energy Variability	
	Pre	Post	Pre	Post	Pre	Post	Pre	Post
P1	0.0005	0.0011 ↑	0.0004	0.0012 ↑	0.0004	0.0013 ↑	563.1547	1736.5020 ↑
P2	0.0048	0.0004 ↓	0.0041	0.0000 ↓	0.0039	0.0001 ↓	6045.7874	89.9957 ↓
P3	0.0027	0.0031 ↑	0.0031	0.0029 ↓	0.0032	0.0029 ↓	4812.9453	3885.2125 ↓
P4	0.0003	0.0069 ↑	0.0004	0.0098 ↑	0.0005	0.0110 ↑	272.9017	4206.8952 ↑
P5	0.0024	0.0054 ↑	0.0024	0.0070 ↑	0.0024	0.0075 ↑	3442.8167	9758.2279 ↑
P6	0.0019	0.0053 ↑	0.0023	0.0060 ↑	0.0024	0.0061 ↑	3138.8382	7802.8106 ↑
P7	0.0016	0.0027 ↑	0.0018	0.0029 ↑	0.0018	0.0029 ↑	2383.3320	3873.4247 ↑
P8	0.0046	0.0003 ↓	0.0050	0.0004 ↓	0.0051	0.0007 ↓	7638.1972	592.6644 ↓
P9	0.0005	0.0022 ↑	0.0005	0.0025 ↑	0.0005	0.0026 ↑	678.2271	3346.5152 ↑
P10	0.0033	0.0044 ↑	0.0032	0.0052 ↑	0.0032	0.0055 ↑	1356.9772	2348.8279 ↑
P11	0.0022	0.0017 ↓	0.0037	0.0011 ↓	0.0044	0.0009 ↓	4898.6972	1605.8169 ↓
P12	0.0008	0.0009 ↑	0.0014	0.0004 ↓	0.0016	0.0003 ↓	1787.0444	660.2686 ↓
P13	0.0007	0.0016 ↑	0.0007	0.0022 ↑	0.0007	0.0023 ↑	1001.6915	2964.7163 ↑

a: The variability in the whole brain regions.
↑: Increased (or equal) variability in the Post stage compared with that in the Pre stage.
↓: Decreased variability in the Post stage compared with that in the Pre stage.

with brainstem hemorrhage (P8, P9), brainstem infarction (P10, P11), and trauma (P12) exhibited no variations. The consciousness states of patients P3, P4, and P6 were changed from vegetative state to minimally conscious state minus while other patients showed no changes of consciousness states. All patients exhibited stable vital signs after DBS surgery and had no postoperative bleeding or infarction. During the experiments, none of patients exhibited eye movements in response to the auditory stimuli.

B. Analysis of Dynamic Brain Temporal-Spectral Features

The global efficiency variability, local efficiency variability (in the whole brain regions), clustering coefficient variability (in the whole brain regions), and graph energy variability in the Pre and Post stages were shown in Table III. The global efficiency variability of ten patients (P1, P3, P4, P5, P6, P7, P9, P10, P12, P13) in the Post stage was consistently higher than that in the Pre stage while three patients (P2, P8, P11) under the Post stage exhibited decrease variations compared with those under the Pre stage. Eight patients (P1, P4, P5, P6, P7, P9, P10, P13) showed consistent treatment-induced increases of local efficiency variability, clustering variability, and graph energy variability while five patients (P2, P3, P8, P11, P12) had opposite variations. The results showed that DOC patients exhibited increased functional variability after DBS treatment.

The local efficiency variability, clustering coefficient variability, and graph diversity variability of different brain regions under the Pre and Post stages were presented in Table IV, V, and VI. The local efficiency variability and clustering

TABLE IV
THE LOCAL EFFICIENCY VARIABILITY IN DIFFERENT BRAIN REGIONS UNDER THE PRE AND POST STAGES

Patient	$V_{LE_{L-FL}}{}^{a}$		$V_{LE_{R-FL}}$		$V_{LE_{L-PL}}$		$V_{LE_{R-PL}}$		$V_{LE_{L-OL}}$		$V_{LE_{R-OL}}$	
	Pre	Post	Pre	Post	Pre	Post	Pre	Post	Pre	Post	Pre	Post
P1	0.0007	0.0014 ↑	0.0009	0.0047 ↑	0.0008	0.0003 ↓	0.0008	0.0014 ↑	0.0012	0.0034 ↑	0.0004	0.0022 ↑
P2	0.0028	0.0003 ↓	0.0051	0.0002 ↓	0.0043	0.0002 ↓	0.0033	0.0006 ↓	0.0075	0.0003 ↓	0.0052	0.0007 ↓
P3	0.0101	0.0036 ↓	0.0025	0.0057 ↑	0.0071	0.0022 ↓	0.0008	0.0025 ↑	0.0005	0.0011 ↑	0.0025	0.0038 ↑
P4	0.0010	0.0094 ↑	0.0012	0.0151 ↑	0.0000	0.0022 ↑	0.0001	0.0177 ↑	-	-	-	-
P5	0.0044	0.0057 ↑	0.0027	0.0066 ↑	0.0030	0.0148 ↑	0.0035	0.0049 ↑	0.0082	0.0109 ↑	0.0042	0.0061 ↑
P6	0.0025	0.0085 ↑	0.0008	0.0074 ↑	0.0029	0.0105 ↑	0.0014	0.0027 ↑	0.0091	0.0064 ↓	0.0041	0.0041 ↑
P7	0.0017	0.0033 ↑	0.0031	0.0061 ↑	0.0020	0.0020 ↑	0.0030	0.0021 ↓	0.0008	0.0036 ↑	0.0018	0.0030 ↑
P8	0.0097	0.0014 ↓	0.0047	0.0001 ↓	0.0030	0.0012 ↓	0.0050	0.0010 ↓	0.0142	0.0025 ↓	0.0002	0.0003 ↑
P9	0.0021	0.0025 ↑	0.0004	0.0014 ↑	0.0012	0.0030 ↑	0.0017	0.0039 ↑	0.0008	0.0016 ↑	0.0016	0.0044 ↑
P10	0.0019	0.0043 ↑	0.0033	0.0067 ↑	0.0061	0.0048 ↓	0.0033	0.0059 ↑	-	-	-	-
P11	0.0051	0.0003 ↓	0.0018	0.0050 ↑	0.0033	0.0019 ↓	0.0036	0.0002 ↓	0.0073	0.0033 ↓	0.0043	0.0013 ↓
P12	0.0006	0.0018 ↑	0.0019	0.0003 ↓	0.0027	0.0006 ↓	0.0049	0.0003 ↓	0.0022	0.0005 ↓	0.0004	0.0007 ↑
P13	0.0003	0.0027 ↑	0.0009	0.0023 ↑	0.0008	0.0020 ↑	0.0018	0.0086 ↑	0.0010	0.0035 ↑	0.0035	0.0023 ↓

a: FL, PL, and OL denote the frontal lobe, parietal lobe, and occipital lobe, respectively. L and R indicate the left and right sides of the brain regions.
↑: Increased (or equal) variability in the Post stage compared with that in the Pre stage.
↓: Decreased variability in the Post stage compared with that in the Pre stage.

TABLE V
THE CLUSTERING COEFFICIENT VARIABILITY IN DIFFERENT BRAIN REGIONS UNDER THE PRE AND POST STAGES

Patient	$V_{CC_{L-FL}}{}^{a}$		$V_{CC_{R-FL}}$		$V_{CC_{L-PL}}$		$V_{CC_{R-PL}}$		$V_{CC_{L-OL}}$		$V_{CC_{R-OL}}$	
	Pre	Post	Pre	Post	Pre	Post	Pre	Post	Pre	Post	Pre	Post
P1	0.0006	0.0015 ↑	0.0008	0.0046 ↑	0.0007	0.0004 ↓	0.0006	0.0015 ↑	0.0009	0.0026 ↑	0.0004	0.0023 ↑
P2	0.0026	0.0001 ↓	0.0047	0.0003 ↓	0.0040	0.0002 ↓	0.0032	0.0003 ↓	0.0069	0.0002 ↓	0.0048	0.0007 ↓
P3	0.0092	0.0036 ↓	0.0026	0.0055 ↑	0.0066	0.0023 ↓	0.0010	0.0023 ↑	0.0010	0.0012 ↑	0.0023	0.0036 ↑
P4	0.0011	0.0104 ↑	0.0013	0.0163 ↑	0.0001	0.0032 ↑	0.0002	0.0185 ↑	-	-	-	-
P5	0.0040	0.0060 ↑	0.0026	0.0073 ↑	0.0029	0.0148 ↑	0.0033	0.0053 ↑	0.0074	0.0109 ↑	0.0039	0.0064 ↑
P6	0.0026	0.0082 ↑	0.0010	0.0073 ↑	0.0028	0.0097 ↑	0.0016	0.0031 ↑	0.0081	0.0064 ↓	0.0040	0.0042 ↑
P7	0.0017	0.0033 ↑	0.0029	0.0056 ↑	0.0021	0.0021 ↑	0.0029	0.0021 ↓	0.0008	0.0034 ↑	0.0019	0.0028 ↑
P8	0.0094	0.0017 ↓	0.0046	0.0002 ↓	0.0034	0.0010 ↓	0.0052	0.0012 ↓	0.0131	0.0028 ↓	0.0004	0.0004 ↑
P9	0.0019	0.0026 ↑	0.0003	0.0016 ↑	0.0010	0.0030 ↑	0.0015	0.0038 ↑	0.0007	0.0018 ↑	0.0013	0.0041 ↑
P10	0.0020	0.0047 ↑	0.0033	0.0069 ↑	0.0057	0.0048 ↓	0.0033	0.0063 ↑	-	-	-	-
P11	0.0056	0.0004 ↓	0.0024	0.0042 ↑	0.0041	0.0016 ↓	0.0043	0.0002 ↓	0.0074	0.0026 ↓	0.0049	0.0012 ↓
P12	0.0007	0.0013 ↑	0.0019	0.0002 ↓	0.0028	0.0006 ↓	0.0049	0.0003 ↓	0.0023	0.0005 ↓	0.0005	0.0003 ↓
P13	0.0004	0.0022 ↑	0.0009	0.0023 ↑	0.0007	0.0023 ↑	0.0016	0.0078 ↑	0.0009	0.0036 ↑	0.0030	0.0023 ↓

a: FL, PL, and OL denote the frontal lobe, parietal lobe, and occipital lobe, respectively. L and R indicate the left and right sides of the brain regions.
↑: Increased (or equal) variability in the Post stage compared with that in the Pre stage.
↓: Decreased variability in the Post stage compared with that in the Pre stage.

variability in the Post stage increased in the left frontal lobe (except P2, P3, P8, P11), right frontal lobe (except P2, P8, P12), left parietal lobe (except P1, P2, P3, P8, P10, P11, P12), right parietal lobe (except P2, P7, P8, P11, P12), and left occipital lobe (except P2, P6, P8, P11, P12) compared with those under the Pre stage. In right occipital lobe, the local efficiency variability (except P2, P11, P13) and clustering variability (except P2, P11, P12, P13) in the Post stage increased compared with those under the Pre stage. Moreover, the graph diversity variability in the Post stage increased the left frontal lobe (except P3, P9, P10, P11, P12), right frontal lobe (except P3, P4, P9, P10, P11, P12), left parietal lobe (except P3, P6, P9, P10, P11, P12, P13), right parietal lobe (except P3, P9, P10, P11, P12, P13), left occipital lobe (except P3, P7, P9, P12), and right occipital lobe (except P1, P3, P6, P7, P9, P12, P13) compared with those under the Pre stage. The variability in the right brain regions had better consistent performance than that in the left brain regions.

C. Correlation Analysis of Dynamic Brain Temporal-Spectral Features and CRS-R Index

The correlations between changes of CRS-R index and changes of global efficiency variability, local efficiency variability (in the whole brain regions), clustering coefficient variability (in the whole brain regions), and graph energy variability were presented in Figure 4. The changes of local efficiency variability and clustering coefficient were significantly correlated with the changes of CRS-R index. The results showed that the consciousness improvements of DOC patients were significantly associated with functional variability.

The correlations between changes of CRS-R index and changes of local efficiency variability, clustering efficiency variability, graph diversity variability in different brain regions were shown in Figure 5 and Table VII. The changes of local efficiency variability and clustering coefficient variability in the right frontal lobe and parietal lobe as well as graph diversity variability in the right occipital lobe were significantly

TABLE VI
THE GRAPH DIVERSITY VARIABILITY IN DIFFERENT BRAIN REGIONS UNDER THE PRE AND POST STAGES

Patient	VGD_{L-FL} [a]		VGD_{R-FL}		VGD_{L-PL}		VGD_{R-PL}		VGD_{L-OL}		VGD_{R-OL}	
	Pre	Post	Pre	Post	Pre	Post	Pre	Post	Pre	Post	Pre	Post
P1	0.0003	0.0004 ↑	0.0002	0.0003 ↑	0.0002	0.0003 ↑	0.0002	0.0005 ↑	0.0003	0.0002 ↑	0.0003	0.0002 ↓
P2	0.0001	0.0003 ↑	0.0002	0.0002 ↑	0.0002	0.0014 ↑	0.0001	0.0007 ↑	0.0002	0.0008 ↑	0.0004	0.0007 ↑
P3	0.0023	0.0000 ↓	0.0021	0.0000 ↓	0.0018	0.0001 ↓	0.0024	0.0002 ↓	0.0020	0.0002 ↓	0.0031	0.0003 ↓
P4	0.0008	0.0014 ↑	0.0013	0.0009 ↓	0.0006	0.0012 ↑	0.0008	0.0016 ↑	-	-	-	-
P5	0.0007	0.0008 ↑	0.0010	0.0014 ↑	0.0010	0.0011 ↑	0.0009	0.0012 ↑	0.0018	0.0020 ↑	0.0016	0.0022 ↑
P6	0.0002	0.0005 ↑	0.0003	0.0003 ↑	0.0004	0.0003 ↓	0.0004	0.0004 ↑	0.0004	0.0005 ↑	0.0017	0.0006 ↓
P7	0.0003	0.0009 ↑	0.0002	0.0005 ↑	0.0002	0.0009 ↑	0.0003	0.0005 ↑	0.0004	0.0003 ↓	0.0004	0.0002 ↓
P8	0.0002	0.0006 ↑	0.0003	0.0006 ↑	0.0002	0.0005 ↑	0.0002	0.0008 ↑	0.0005	0.0010 ↑	0.0010	0.0013 ↑
P9	0.0014	0.0001 ↓	0.0014	0.0002 ↓	0.0009	0.0001 ↓	0.0011	0.0002 ↓	0.0010	0.0003 ↓	0.0013	0.0004 ↓
P10	0.0010	0.0003 ↓	0.0012	0.0001 ↓	0.0026	0.0003 ↓	0.0009	0.0004 ↓	-	-	-	-
P11	0.0005	0.0002 ↓	0.0004	0.0001 ↓	0.0003	0.0005 ↓	0.0007	0.0001 ↓	0.0002	0.0006 ↑	0.0004	0.0007 ↑
P12	0.0026	0.0006 ↓	0.0021	0.0007 ↓	0.0018	0.0009 ↓	0.0016	0.0011 ↓	0.0023	0.0011 ↓	0.0021	0.0008 ↓
P13	0.0003	0.0006 ↑	0.0002	0.0006 ↑	0.0005	0.0004 ↓	0.0005	0.0004 ↓	0.0002	0.0009 ↑	0.0006	0.0004 ↓

a: FL, PL, and OL denote the frontal lobe, parietal lobe, and occipital lobe, respectively. L and R indicate the left and right sides of the brain regions.
↑: Increased (or equal) variability in the Post stage compared with that in the Pre stage.
↓: Decreased variability in the Post stage compared with that in the Pre stage.

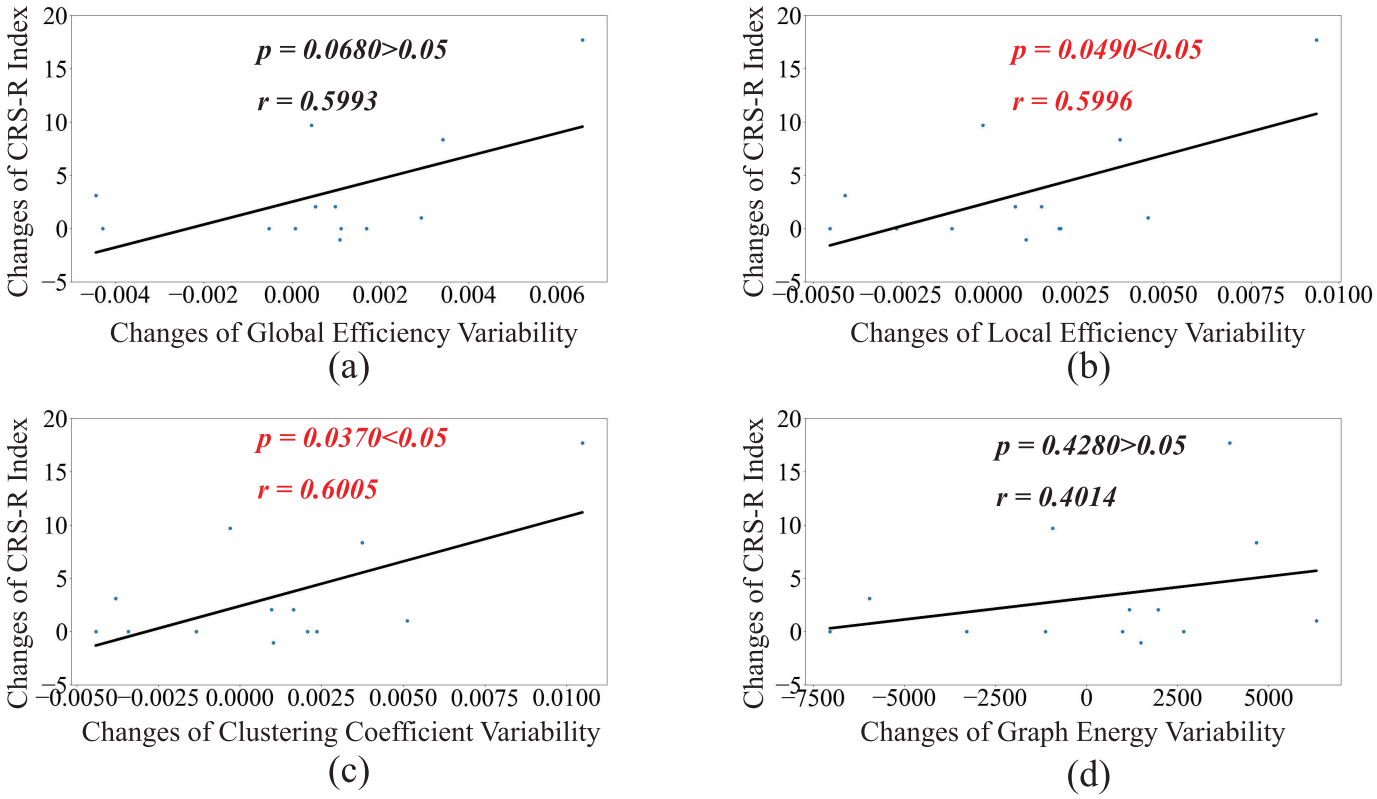

Fig. 4. Correlation between changes of CRS-R index and changes of global efficiency variability (a), local efficiency variability in the whole brain regions (b), clustering coefficient variability in the whole brain regions (c), and graph energy variability (d). Red denotes significant correlation. *p* and *r* indicate the p-value and correlation strength.

correlated with the changes of CRS-R index, indicating that consciousness improvements of DOC patients were significantly associated with the variability in the right hemisphere.

The above results found that: (1) The increases of functional variability were significantly correlated with the improvements of consciousness. (2) The functional variability in the right brain regions had stronger correlations with consciousness enhancements than that in the left brain regions.

IV. DISCUSSION

Dynamic brain networks characterized the temporal variations of brain networks and were critical for the exploration of cognitive, behavioral, and physiological processes [48], [49], [50]. Network variability was a crucial property of dynamic brain networks and associated with cognitive task performance [45], [51], [52]. In this study, an analysis method was proposed to discover dynamic brain temporal-spectral

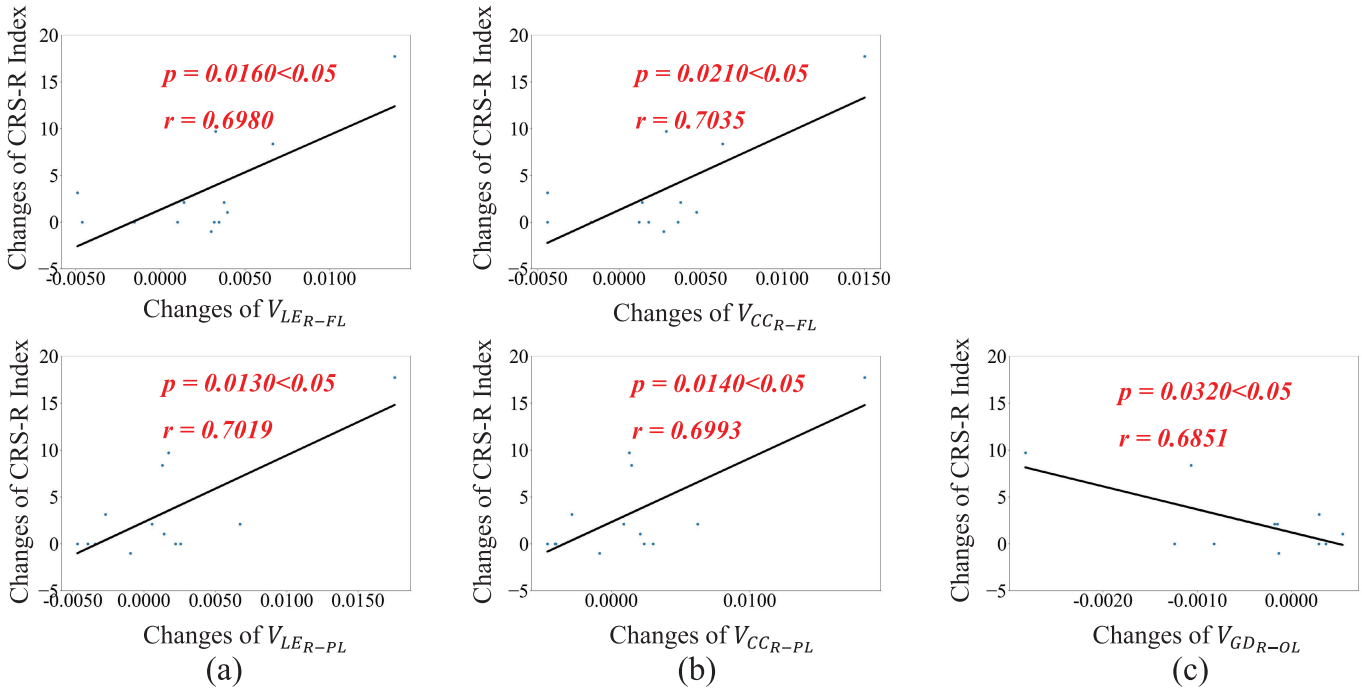

Fig. 5. Significant correlation between changes of CRS-R index and (a) changes of the local efficiency variability in the right frontal lobe $V_{LE_{R-FL}}$ and parietal lobe $V_{LE_{R-PL}}$, (b) clustering coefficient variability in the right frontal lobe $V_{CC_{R-FL}}$ and parietal lobe $V_{CC_{R-PL}}$, (c) and graph diversity variability in the right occipital lobe $V_{GD_{R-OL}}$. Red denotes significant correlation. *p* and *r* indicate the p-value and correlation strength.

TABLE VII
CORRELATION ANALYSIS BETWEEN THE CHANGES OF CRS-R INDEX AND CHANGES OF LOCAL EFFICIENCY VARIABILITY, CLUSTERING COEFFICIENT VARIABILITY, AND GRAPH DIVERSITY VARIABILITY IN DIFFERENT BRAIN REGIONS. THE NUMBER REPRESENTS P-VALUE. RED DENOTES SIGNIFICANT CORRELATION ($p < 0.05$)

Brain Regions	$V_{LE_{Re}}$	$V_{CC_{Re}}$	$V_{GD_{Re}}$
Left Frontal Lobe (L-FL)	0.0840	0.0850	0.4800
Right Frontal Lobe (R-FL)	**0.0160**	**0.0210**	0.3840
Left Parietal Lobe (L-PL)	0.3770	0.3220	0.6830
Right Parietal Lobe (R-PL)	**0.0130**	**0.0140**	0.2030
Left Occipital Lobe (L-OL)	0.7690	0.6750	0.2970
Right Occipital Lobe (R-OL)	0.8370	0.8460	**0.0320**

features, which quantified the variability in the temporal and spectral representations of brain functional networks.

Our study showed that DOC patients exhibited an increase of network variability and consciousness improvements after DBS treatment. Previous studies found that patients with Parkinson's disease had a decrease of network variability compared with healthy controls [53], suggesting that decreased network variability was correlated with the impairment of motor and cognitive functions. In [54], patients with schizophrenia had decreased variance in the dynamic graph metrics in comparison to healthy controls, showing that the impairment of mental functions could be reflected by the decrease of network variability. In [34], Cai et al. found decreased temporal fluctuations of global metrics in DOC patients compared to the healthy controls. In [55], Lee et al. demonstrated that the reduced diversity of functional connectivity patterns was associated with the loss of consciousness. In line with these studies, Lee et al. explored the relationships between the temporal diversity of phase synchronization and critical dynamics [56]. They reported that the brain networks with low diversity were away from the normal critical point. Our study was consistent with the results, demonstrating the significant correlation between enhanced network variability and improved consciousness.

Our study showed that the right brain regions of DOC patients were better improved by DBS compared with the left brain regions. In [57], Arnts et al. found that DBS was associated with the increase of functional connectivity among DOC patients in frontoparietal and occipital areas, especially within the right brain regions. This finding suggested that the increased connectivity in the right brain regions was more correlated with the consciousness improvements of DOC patients than that in the left brain regions. In [58], the complexity of neural activities between regions in the right hemisphere exhibited a significantly stronger correlation with CRS-R compared with that between regions in the left hemisphere, which was in line with our results. One potential explanation for our finding is that the brain regions in the right hemisphere primarily engage in interactions with components of the ascending arousal system. These interactions are responsible for regulating behavioral arousal, consciousness, and motivation, as they receive and process information from this system [59]. Therefore, the variability features in the right brain regions may achieve better reflections of the consciousness-related brain functional variations than those in the left brain regions.

Another possible explanation is that the right hemisphere may have the potential to promote communication [60], [61], and the extensive preservation of functionality in the right cerebral hemisphere among DOC patients could indicate a motivation for communication [62]. The maintained functionality in the right hemisphere, as opposed to the left hemisphere, may be crucial in initiating attention to verbal stimulation and facilitating communication. In DOC patients, motivation to engage in communication related to the right hemisphere is paramount and may precede the execution of verbal and motor functions during communication involving the left hemisphere. Our study was consistent with the above results, demonstrating that the right brain regions had a stronger correlation with consciousness improvements of DOC patients than the left brain regions.

We hope this work can encourage more study, and more clinical evidence will promisingly enable quantified and individualized optimization of DBS therapy for each DOC patient. This work also had the potential to enable objective analysis of rehabilitation, medication, and surgical treatment of other brain disorders, such as stroke and Parkinson's disease, by providing definitive evidence in the neural functional levels. The sham stimuli will be explored in the future. Moreover, in the future, we will consider trying to record multiple trials.

V. Conclusion

The evaluation of consciousness variations plays a critical role in the treatment optimization of DBS therapy for DOC patients. This paper proposed an analysis method for the effectiveness evaluation and mechanism exploration of DBS and discovered that dynamic brain temporal-spectral features well signified DBS-induced brain functional variations and could be applied to evaluate consciousness in DOC patients. Dynamic brain temporal-spectral features were extracted for the assessment of global and local functional variability before and after DBS treatment. The results showed that the brain temporal-spectral functional variability was promising for consciousness assessment in DOC patients.

References

[1] B. L. Edlow, J. Claassen, N. D. Schiff, and D. M. Greer, "Recovery from disorders of consciousness: Mechanisms, prognosis and emerging therapies," *Nature Rev. Neurol.*, vol. 17, no. 3, pp. 135–156, Mar. 2021.

[2] C. Schnakers and M. M. Monti, "Towards improving care for disorders of consciousness," *Nature Rev. Neurol.*, vol. 16, no. 8, pp. 405–406, Aug. 2020.

[3] M. M. Monti et al., "Willful modulation of brain activity in disorders of consciousness," *New England J. Med.*, vol. 362, no. 7, pp. 579–589, Feb. 2010.

[4] A. M. Owen, "Improving diagnosis and prognosis in disorders of consciousness," *Brain*, vol. 143, no. 4, pp. 1050–1053, Apr. 2020.

[5] J. Stender et al., "Diagnostic precision of PET imaging and functional MRI in disorders of consciousness: A clinical validation study," *Lancet*, vol. 384, no. 9942, pp. 514–522, Aug. 2014.

[6] A. Rezaei Haddad, V. Lythe, and A. L. Green, "Deep brain stimulation for recovery of consciousness in minimally conscious patients after traumatic brain injury: A systematic review," *Neuromodulation, Technol. Neural Interface*, vol. 22, no. 4, pp. 373–379, Jun. 2019.

[7] J. K. Krauss et al., "Technology of deep brain stimulation: Current status and future directions," *Nature Rev. Neurol.*, vol. 17, no. 2, pp. 75–87, Feb. 2021.

[8] N. D. Schiff et al., "Behavioural improvements with thalamic stimulation after severe traumatic brain injury," *Nature*, vol. 448, no. 7153, pp. 600–603, Aug. 2007.

[9] L. Magrassi et al., "Results of a prospective study (CATS) on the effects of thalamic stimulation in minimally conscious and vegetative state patients," *J. Neurosurgery*, vol. 125, no. 4, pp. 972–981, Oct. 2016.

[10] Y. Yang et al., "Long-term functional outcomes improved with deep brain stimulation in patients with disorders of consciousness," *Stroke Vascular Neurol.*, vol. 8, no. 5, pp. 368–378, Oct. 2023.

[11] A. Thibaut, N. Schiff, J. Giacino, S. Laureys, and O. Gosseries, "Therapeutic interventions in patients with prolonged disorders of consciousness," *Lancet Neurol.*, vol. 18, no. 6, pp. 600–614, Jun. 2019.

[12] D. Sattin et al., "Effect of rehabilitation treatments on disability in persons with disorders of consciousness: A propensity score study," *Arch. Phys. Med. Rehabil.*, vol. 101, no. 1, pp. 95–105, Jan. 2020.

[13] M. E. Barra, B. L. Edlow, and G. M. Brophy, "Pharmacologic therapies to promote recovery of consciousness," *Seminars Neurol.*, vol. 42, no. 3, pp. 335–347, 2022.

[14] J. Vanhoecke and M. Hariz, "Deep brain stimulation for disorders of consciousness: Systematic review of cases and ethics," *Brain Stimulation*, vol. 10, no. 6, pp. 1013–1023, Nov. 2017.

[15] J. T. Giacino, K. Kalmar, and J. Whyte, "The JFK coma recovery scale-revised: Measurement characteristics and diagnostic utility," *Arch. Phys. Med. Rehabil.*, vol. 85, no. 12, pp. 2020–2029, 2004.

[16] S. Frigerio et al., "Neuropsychological assessment through coma recovery scale-revised and coma/near coma scale in a sample of pediatric patients with disorder of consciousness," *J. Neurol.*, vol. 270, no. 2, pp. 1019–1029, Feb. 2023.

[17] J. Annen et al., "Diagnostic accuracy of the CRS-R index in patients with disorders of consciousness," *Brain Injury*, vol. 33, no. 11, pp. 1409–1412, Sep. 2019.

[18] N. D. Schiff, "Central thalamic deep brain stimulation to support anterior forebrain mesocircuit function in the severely injured brain," *J. Neural Transmiss.*, vol. 123, no. 7, pp. 797–806, Jul. 2016.

[19] J. Lemaire et al., "Deep brain stimulation in five patients with severe disorders of consciousness," *Ann. Clin. Transl. Neurol.*, vol. 5, no. 11, pp. 1372–1384, Nov. 2018.

[20] B. Kundu, A. A. Brock, D. J. Englot, C. R. Butson, and J. D. Rolston, "Deep brain stimulation for the treatment of disorders of consciousness and cognition in traumatic brain injury patients: A review," *Neurosurgical Focus*, vol. 45, no. 2, p. E14, Aug. 2018.

[21] Y. Dang et al., "Deep brain stimulation improves electroencephalogram functional connectivity of patients with minimally conscious state," *CNS Neurosci. Therapeutics*, vol. 29, no. 1, pp. 344–353, Jan. 2023.

[22] R. K. Almajidy, K. Mankodiya, M. Abtahi, and U. G. Hofmann, "A Newcomer's guide to functional near infrared spectroscopy experiments," *IEEE Rev. Biomed. Eng.*, vol. 13, pp. 292–308, 2020.

[23] P. Pinti et al., "The present and future use of functional near-infrared spectroscopy (fNIRS) for cognitive neuroscience," *Ann. New York Acad. Sci.*, vol. 1464, no. 1, pp. 5–29, Mar. 2020.

[24] M. Mahmoudzadeh, F. Wallois, M. Tir, P. Krystkowiak, and M. Lefranc, "Cortical hemodynamic mapping of subthalamic nucleus deep brain stimulation in parkinsonian patients, using high-density functional near-infrared spectroscopy," *PLoS ONE*, vol. 16, no. 1, Jan. 2021, Art. no. e0245188.

[25] N. Yu et al., "Quantified assessment of deep brain stimulation on Parkinson's patients with task fNIRS measurements and functional connectivity analysis: A pilot study," *Chin. Neurosurgical J.*, vol. 7, no. 1, pp. 171–181, Jul. 2021.

[26] M. Li et al., "Detecting residual awareness in patients with prolonged disorders of consciousness: An fNIRS study," *Frontiers Neurol.*, vol. 12, Jul. 2021, Art. no. 618055.

[27] A. Abdalmalak, D. Milej, L. Norton, D. B. Debicki, A. M. Owen, and K. S. Lawrence, "The potential role of fNIRS in evaluating levels of consciousness," *Frontiers Hum. Neurosci.*, vol. 15, Jul. 2021, Art. no. 703405.

[28] J. Si et al., "Evaluation of residual cognition in patients with disorders of consciousness based on functional near-infrared spectroscopy," *Neurophotonics*, vol. 10, no. 2, Apr. 2023, Art. no. 025003.

[29] Z. Shu et al., "FNIRS-based functional connectivity signifies recovery in patients with disorders of consciousness after DBS treatment," *Clin. Neurophysiol.*, vol. 147, pp. 60–68, Mar. 2023.

[30] J. Lu et al., "An fNIRS-based dynamic functional connectivity analysis method to signify functional neurodegeneration of Parkinson's disease," *IEEE Trans. Neural Syst. Rehabil. Eng.*, vol. 31, pp. 1199–1207, 2023.

[31] T. Yan et al., "Effects of microstate dynamic brain network disruption in different stages of schizophrenia," *IEEE Trans. Neural Syst. Rehabil. Eng.*, vol. 31, pp. 2688–2697, 2023.

[32] A. Naro et al., "Shedding new light on disorders of consciousness diagnosis: The dynamic functional connectivity," *Cortex*, vol. 103, pp. 316–328, Jun. 2018.

[33] R. Panda et al., "Disruption in structural–functional network repertoire and time-resolved subcortical fronto-temporoparietal connectivity in disorders of consciousness," *Elife*, vol. 11, Aug. 2022, Art. no. e77462.

[34] L. Cai, J. Wang, Y. Guo, M. Lu, Y. Dong, and X. Wei, "Altered inter-frequency dynamics of brain networks in disorder of consciousness," *J. Neural Eng.*, vol. 17, no. 3, Jun. 2020, Art. no. 036006.

[35] A. López-González et al., "Loss of consciousness reduces the stability of brain hubs and the heterogeneity of brain dynamics," *Commun. Biol.*, vol. 4, no. 1, p. 1037, Sep. 2021.

[36] A. Horn et al., "Lead-DBS v2: Towards a comprehensive pipeline for deep brain stimulation imaging," *NeuroImage*, vol. 184, pp. 293–316, Jan. 2019.

[37] L. Wojtecki et al., "Modulation of central thalamic oscillations during emotional-cognitive processing in chronic disorder of consciousness," *Cortex*, vol. 60, pp. 94–102, Nov. 2014.

[38] A. Thul et al., "EEG entropy measures indicate decrease of cortical information processing in disorders of consciousness," *Clin. Neurophysiol.*, vol. 127, no. 2, pp. 1419–1427, Feb. 2016.

[39] J. Zhu et al., "Clinical research: Auditory stimulation in the disorders of consciousness," *Frontiers Hum. Neurosci.*, vol. 13, p. 324, Sep. 2019.

[40] F. Scholkmann, S. Spichtig, T. Muehlemann, and M. Wolf, "How to detect and reduce movement artifacts in near-infrared imaging using moving standard deviation and spline interpolation," *Physiolog. Meas.*, vol. 31, no. 5, p. 649, 2010.

[41] Y. J. Wu et al., "Rapid learning of a phonemic discrimination in the first hours of life," *Nature Hum. Behav.*, vol. 6, no. 8, pp. 1169–1179, Jun. 2022.

[42] Y.-L. Zheng, D.-X. Wang, Y.-R. Zhang, and Y.-Y. Tang, "Enhancing attention by synchronizing respiration and fingertip pressure: A pilot study using functional near-infrared spectroscopy," *Frontiers Neurosci.*, vol. 13, p. 1209, Nov. 2019.

[43] X. Si, S. Li, S. Xiang, J. Yu, and D. Ming, "Imagined speech increases the hemodynamic response and functional connectivity of the dorsal motor cortex," *J. Neural Eng.*, vol. 18, no. 5, Oct. 2021, Art. no. 056048.

[44] D. T. Delpy, M. Cope, P. V. D. Zee, S. Arridge, S. Wray, and J. Wyatt, "Estimation of optical pathlength through tissue from direct time of flight measurement," *Phys. Med. Biol.*, vol. 33, no. 12, pp. 1433–1442, Dec. 1988.

[45] D. D. Garrett, N. Kovacevic, A. R. McIntosh, and C. L. Grady, "The modulation of BOLD variability between cognitive states varies by age and processing speed," *Cerebral Cortex*, vol. 23, no. 3, pp. 684–693, Mar. 2013.

[46] W. Huang, L. Goldsberry, N. F. Wymbs, S. T. Grafton, D. S. Bassett, and A. Ribeiro, "Graph frequency analysis of brain signals," *IEEE J. Sel. Topics Signal Process.*, vol. 10, no. 7, pp. 1189–1203, Oct. 2016.

[47] A. Ortega, P. Frossard, J. Kovacevic, J. M. F. Moura, and P. Vandergheynst, "Graph signal processing: Overview, challenges, and applications," *Proc. IEEE*, vol. 106, no. 5, pp. 808–828, May 2018.

[48] Z. Huang, J. Zhang, J. Wu, G. A. Mashour, and A. G. Hudetz, "Temporal circuit of macroscale dynamic brain activity supports human consciousness," *Sci. Adv.*, vol. 6, no. 11, Mar. 2020, Art. no. eaaz0087.

[49] V. Sip, M. Hashemi, T. Dickscheid, K. Amunts, S. Petkoski, and V. Jirsa, "Characterization of regional differences in resting-state fMRI with a data-driven network model of brain dynamics," *Sci. Adv.*, vol. 9, no. 11, Mar. 2023, Art. no. eabq7547.

[50] G. Yi et al., "Capturing the abnormal brain network activity in early Parkinsons disease with mild cognitive impairment based on dynamic functional connectivity," *IEEE Trans. Neural Syst. Rehabil. Eng.*, vol. 31, pp. 1238–1247, 2023.

[51] Y. Long et al., "Altered temporal variability of local and large-scale resting-state brain functional connectivity patterns in schizophrenia and bipolar disorder," *Frontiers Psychiatry*, vol. 11, p. 422, May 2020.

[52] E. T. Rolls, W. Cheng, and J. Feng, "Brain dynamics: The temporal variability of connectivity, and differences in schizophrenia and ADHD," *Transl. Psychiatry*, vol. 11, no. 1, p. 70, Jan. 2021.

[53] J. Cai et al., "Dynamic graph theoretical analysis of functional connectivity in Parkinson's disease: The importance of Fiedler value," *IEEE J. Biomed. Health Informat.*, vol. 23, no. 4, pp. 1720–1729, Jul. 2019.

[54] Q. Yu et al., "Assessing dynamic brain graphs of time-varying connectivity in fMRI data: Application to healthy controls and patients with schizophrenia," *NeuroImage*, vol. 107, pp. 345–355, Feb. 2015.

[55] H. Lee et al., "Diversity of functional connectivity patterns is reduced in propofol-induced unconsciousness," *Hum. Brain Mapping*, vol. 38, no. 10, pp. 4980–4995, Oct. 2017.

[56] H. Lee et al., "Relationship of critical dynamics, functional connectivity, and states of consciousness in large-scale human brain networks," *NeuroImage*, vol. 188, pp. 228–238, Mar. 2019.

[57] H. Arnts et al., "Clinical and neurophysiological effects of central thalamic deep brain stimulation in the minimally conscious state after severe brain injury," *Sci. Rep.*, vol. 12, no. 1, p. 12932, Jul. 2022.

[58] Y. Liu, W. Zeng, N. Pan, X. Xia, Y. Huang, and J. He, "EEG complexity correlates with residual consciousness level of disorders of consciousness," *BMC Neurol.*, vol. 23, no. 1, pp. 1–9, Apr. 2023.

[59] O. Boukrina and A. M. Barrett, "Disruption of the ascending arousal system and cortical attention networks in post-stroke delirium and spatial neglect," *Neurosci. Biobehavioral Rev.*, vol. 83, pp. 1–10, Dec. 2017.

[60] A. N. Schore, "Forging connections in group psychotherapy through right brain-to-right brain emotional communications. Part 1: Theoretical models of right brain therapeutic action. Part 2: Clinical case analyses of group right brain regressive enactments," *Int. J. Group Psychotherapy*, vol. 70, no. 1, pp. 29–88, Jan. 2020.

[61] K. M. Hartikainen, "Emotion-attention interaction in the right hemisphere," *Brain Sci.*, vol. 11, no. 8, p. 1006, Jul. 2021.

[62] N. Usami et al., "Cerebral glucose metabolism in patients with chronic disorders of consciousness," *Can. J. Neurolog. Sci./J. Canadien des Sci. Neurologiques*, vol. 50, no. 5, pp. 719–729, Sep. 2023.